



# A Robust PCA-SURE Thresholding Deep Neural Network Approach for Mental Task Brain Computer Interface

Nguyen The Hoang Anh<sup>1,\*</sup>, T. T. Quyen Bui<sup>1</sup>, Nguyen Truong Thang<sup>1</sup>, Thanh Ha Le<sup>2</sup> and The Duy Bui<sup>2</sup>

<sup>1</sup> Institute of Information Technology, Vietnam Academy of Science and Technology, Hanoi, Vietnam

<sup>2</sup> University of Engineering and Technology, Vietnam National University, Hanoi, Vietnam

\*Corresponding author: [nt.hoanganh@ioit.ac.vn](mailto:nt.hoanganh@ioit.ac.vn)

**Abstract.** *Electroencephalographic (EEG) characteristics, i.e., non-linear structure and non-stationarity, make mental state recognition not a trivial task to various classification models. In this paper, a combined principal component analysis (PCA) – Deep neural network approach is proposed as a robust and effective solution to classifying EEG signals recorded with low-cost and portable recording systems into different mental states towards implementation of a Brain computer interface (BCI) capable of controlling electronic devices. Stein’s unbiased risk estimate (SURE) thresholding – PCA is utilized to obtain spectral features that are most essential for deep neural network classifier to perform at best. The contributions of this paper are three-fold. First, we propose a novel, robust and efficient method that integrates SURE thresholding, PCA and Deep Neural Network (DNN), along with other signal processing and machine learning techniques for mental state recognition. Second, a complete mental-task-based BCI using an appropriate experimental design without any assistant equipment is presented. Third, SURE risk thresholding is utilized and proven to be an effective method to automatically determine the appropriate number of principal components of EEG features returned by performing PCA. Experimental results show that our method outperforms others in an EEG dataset of four subjects with highest classification accuracies on dual and triple mental state task experiments of 96.83% and 76.90%, respectively.*

**Keywords.** 62H25; 92B20; 68T27; 92C55

**MSC.** Brain computer interface; Principal component analysis; Deep learning; EEG and SURE thresholding

**Received:** April 24, 2018

**Accepted:** October 13, 2018

## 1. Introduction

A Brain computer interface is a communication system between human and surrounding environment that is implemented based purely on neural activity generated by the brain but any peripheral muscular activity [32]. Neural signals are recorded by various recording modalities, e.g., *magnetic resonance imaging* (MRI), *computed tomography* (CT), *positron emission tomography* (PET), *near infrared spectroscopy* (NIRS), etc. and then translated into useful information or control command representing user's intent [55]. Among those, an *electroencephalogram* (EEG), a recording modality which allows us to record the neural activities in the form of electrical signals with a recording system that consists of electrodes placed across the scalp of the human head, is less expensive and more portable. Due to that reason, EEG is widely used in a broad range of applications [19, 46, 58] from medical treatment to wheelchair control. EEG is a promising way to understand a message that a person with severe physical disabilities (i.e., completely paralyzed patients) delivers to others or expresses what he/she attempts to do. It is desired for decades [13, 15, 30] to build a BCI based on EEG that enables patients to translate a user's intentions into control commands to perform control tasks, i.e., turn on/off electronic devices such as electronic light, fan, television, etc. If such a real time BCI is realizable, it would create an accessible channel for people with severe physical disabilities or patients in critical health condition to communicate with surrounding environment and improve their life quality.

EEG-based BCI can be implemented in a variety of ways whose inputs are P300 event-related potential, *slow cortical potential* (SCP),  $\mu$  (8-13 Hz) and  $\beta$  (14-30 Hz) rhythms, *steady-state visual evoked potentials* (SSVEP), just to name a few [13, 14, 22, 56]. A BCI for word spelling that combines P300-speller confidence with the error-related potential is presented. The system is tested by 11 subjects asked to look at a screen for P300 stimuli generation and then its performance is improved with online error correction [59]. SSVEP are evoked potentials rarely affected by artifacts with low *signal to noise ratio* (SNR) and generated periodically by repeating visual stimulation at frequencies greater than 6 Hz [6, 31]. Lower limb exoskeleton control has successfully been implemented with a SSVEP-based BCI. In this BCI, users are required to gaze at flashing LED light in a long duration that leads to fatigue [26]. SCP is EEG at slow negative voltage shifts occurring over sensorimotor cortex while subjects perform actual or imagined movements. There remain three major disadvantages (weak multidimensional control, training time, and high error probability) with BCIs using SCP that makes it hard for a SCP BCI to be implemented in practice [3].

To overcome these problems, we develop a BCI based on mental state recognition due to its simplicity that does not require assistant equipment (e.g. flashing light board) to be installed as of P300 or SSVEP BCIs. With such a mental-based BCI, users could communicate with surrounding environments independently without any assistants. In the literature, works have been done on mental state recognition that makes BCI possible in this research direction. For instance, in a BCI campaign [10, 37], the subjects are asked to perform three different

mental tasks that are imagination of repetitive self-paced left hand movements, imagination of repetitive self-paced right hand movements, and mental generation of words starting with a letter chosen spontaneously by the subject at the beginning of the task. The highest accuracies of mental task classification reported for this task are 77.3% [10], 76.1% [37], and 68.7% at a BCI competition [7]. The reason that there are different results reported on the same mental task experiment is that the evaluation method is not performed on the same dataset and the recording conditions are not exactly identical which may affect the method performance evaluation. In [4], two mental tasks including baseline measurement and mental multiplication are performed by subjects. The highest classification accuracy of 96.5% is achieved with an *artificial neural network* (ANN) trained with features extracted by multivariate autoregressive models. EEG signals recorded during a pronunciation imagination of four Korean vowels task that could be extracted efficiently for essential features with harmony search and discrete wavelet transform are utilizable for the same purpose at the works of [42].

In our work, an EEG-based BCI is developed for the purpose of controlling electronic devices. Our ultimate purpose is to implement a practical low cost BCI, so we use Emotiv EPOC+, a portable headset that can record quality neural signals. Our BCI setting includes asking the subjects to perform three mental tasks that are neutral – think about nothing, light – imagine light turned on/off, and paper – memorize a sentence from a scientific paper. Brain waves recorded in this manner are well-distinguished so appropriate computational models are capable of interpreting subjects' intents more accurately [5].

Neural engineering algorithms have been developed for an effective solution to mental state classification towards BCI implementation. EEG signals are translated into spectral features and then classified with linear classifiers, i.e., *linear discriminant analysis* (LDA) and *support vector machines* (SVMs), which produces low accurate results. Assumption is made that there exist non-linear and complicated relationships among those features. Therefore, it is not possible for linear classifiers to generate a suitable classifying model. Low accuracies are returned with several statistical methods, i.e., *Naïve Bayesian* (NB) and *K-nearest neighbor* (KNN). As discussed previously, the performance of a BCI could be improved if EEG signals are converted into more essential features in a suitable domain (e.g., spectral domain) and that facilitate machine learning model to perform classification more effectively. Shallow structure ANN with spectral features dimensionality-reduced by PCA is determined to be capable of doing well on this mental state recognition problem [5]. *Deep Neural Network* (DNN) has been successfully implemented in EEG research works such as for recognition of subjects' intents in motor imagery tasks [33,53] and prediction of drivers' cognitive performance [16]. Deep learning layered structure with different levels of abstraction makes it a good candidate to exploit the complicated and non-structural nature of EEG spectral features for effective classification [32].

In this study, we propose a novel approach that combines DNN and PCA-SURE thresholding feature extraction with several main contributions described as follows. First, we propose a novel, robust and efficient method that integrates SURE thresholding, PCA and DNN, along

with other signal processing and machine learning techniques for mental state recognition with highest classification accuracies of 96.77% and 76.98% for dual-mental state (Neutral - Non-neutral) and triple-mental state (Neutral – Light - Paper), respectively on an EEG dataset of four healthy subjects. Experimental results show that our method outperforms other models using SVMs and shallow ANN. Second, that the proposed system requires no assistant equipment, an advantage over other BCIs using P300 or SSVEP, makes it possible to be implemented in real time making it completely possible to implement a BCI to control electronic devices. Third, SURE risk thresholding is utilized to save computational power and improve overall system performance and proven to be an effective method to automatically determine the appropriate number of principal components of EEG features returned by performing PCA. One advantage of SURE risk thresholding is that it is an adaptive method in which the threshold is determined based on characteristics of data.

The rest of the paper is organized as follows: related works are described in Section 2, proposed method is presented in Section 3, experimental results are reported in Section 4, discussion about the experimentation is given in Section 5 and the paper is concluded in Section 6.

## 2. Related Works

### 2.1 Brain Computer Interface Technology

Brain computer interface, an expression coined by J. Vidal in the 1970s, is a non-invasive communication system that requires no peripheral nerves and muscles intermediaries of user [56]. BCIs are necessary systems to assist paralyzed/health-critical condition patients. A BCI consists of a number of sequential sub-blocks that are signal acquisition, signal pre-processing, feature extraction, feature selection/translation, classification, and output device [55]. Hence, the main components to realize a BCI are described as follows:

*Preprocessing:* noises/artifacts caused by non-physiological/physiological factors are removed to eliminate unnecessary information. By doing that, “clean” EEG signals are translated into correct user’s intents more accurately.

*Feature extraction:* Due to unstructured and complicated characteristics, raw EEG signals are not easy to be exploited efficiently. Hence, “clean” signals are converted from time domain to others, i.e., frequency or time-frequency, that provide representation of the original information carried by EEG signals at different domains. The new features are more informative and essential for the following processing steps.

*Feature selection/translation:* features need to be selected in the way that they represent original user’s intents at best and they enable classification models to work more effectively.

*Classification:* This is a crucial step in which machine learning models are in charge of categorizing best-suited features into groups corresponding to user’s intents.

In the following, BCIs based on different technologies/EEG-features are going to be described.

## 2.2 Related BCIs

### i. BCI2000

BCI2000 is a general-purpose, real-time, TCP/IP network protocol based software system that allows conducting research and developing BCI applications with EEG signals [49]. The design of BCI2000 consists of four main modules: operator, source/storage, signal processing and user application as demonstrated in Figure 1. In this structure, the operator module has a graphical interface and bilateral communication with all other modules and acts as a central relay for system configuration and online interaction/data analysis. The source module is integrated with five components including three A/D converters/filters/amplifiers, EEG recording systems and a signal generator for system development and testing. In the Signal processing module, there remain two essential stages: a feature extraction and translation algorithm and an additional statistics component. The last module (user application) has been updated a number of scenarios including four cursor movement, user prospective evaluation, auditory and visual stimuli user-selectable presence, evoked potentials based speller. In most of these applications the BCI needs extra equipment such as screens for EEG signal signature, e.g. P300, elicitation.

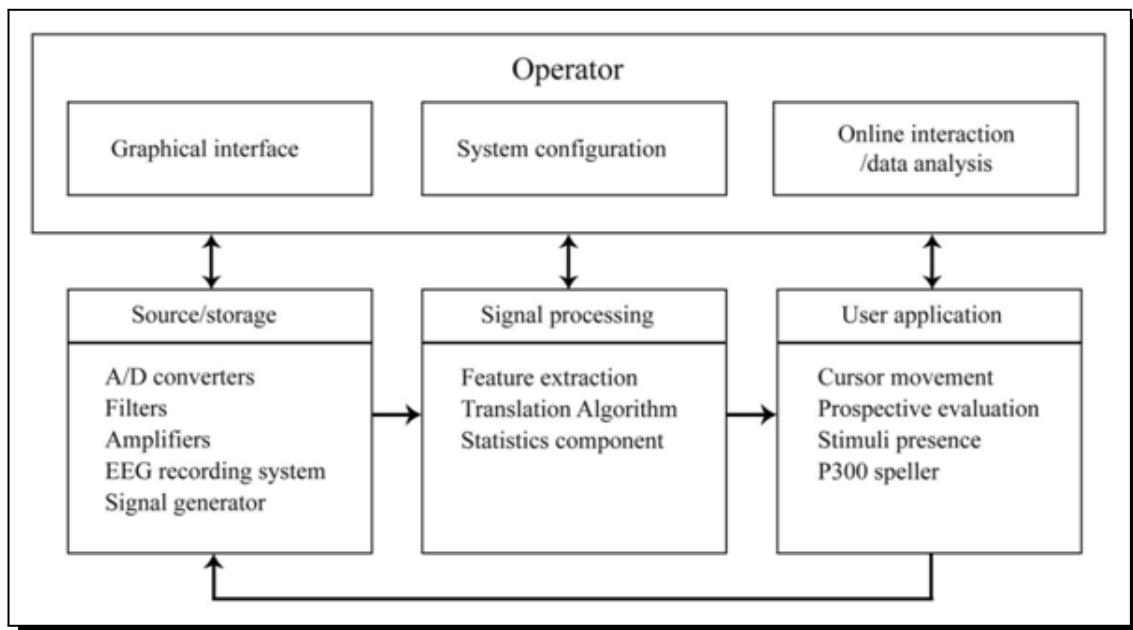
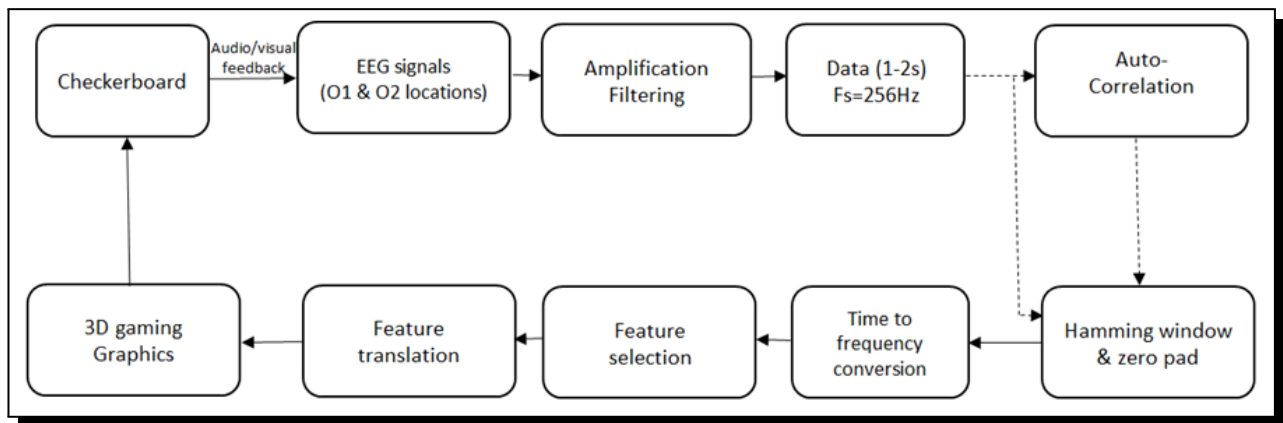


Figure 1. BCI 2000

### ii. SSVEP-based brain computer interface for 3D gaming

*Steady state visually evoked potentials / responses* (SSVEP/R) are natural EEG responses/signals observed after the subjects are visually stimulated at specific frequencies [34]. SSVEP has been developed for different purposes like physical device or computer program operation [36], prosthesis control [39] and attention tracking [23].



**Figure 2.** SSVEP-based BCI for 3D gaming

In this section, a SSVEP-based BCI within a real-time gaming framework aimed at moving an animated character [27] is illustrated. For this BCI experimental setup, subjects are asked to sit in front of a computer screen and their goals are to gain 1D control of an animated character balance. The game attracts more attention with musical soundtrack and character's spoken comments. During the game, a checkerboard is put on either side of the character and phase-reversed at 17 and 20 Hz. This condition requires the subjects to keep attention state of left or right checkerboard for each period of 15 seconds. The player has to ensure the balance of character while he is tightrope walking and stumbles every 1.5-5.0 seconds to one random side. This off-balance status last 3 seconds and evokes subjects' SSVEPs that is necessary for the BCI operation. This SSVEP-based BCI that is integrated in a combined graphics, signal processing and network communications engine. The signal processing pipeline is described as in Figure 2.

### iii. Motor-imagery BCI

*Motor-imagery* (MI) is the description of a mental experiment in which subjects are asked to imagine moving a body part without actual action [33, 53]. While a subject performs MI tasks, the activated regions of his brain are similar to the ones when he realizes such movements. MI-based BCIs is presented in different applications [29, 33, 47, 53]. Recently, a BCI based on *motor-imagery* (MI) approach has been developed and implemented successfully for an incompletely locked-in user with adaptive assistance [47]. In this BCI setting protocol, different movement imaginations are conducted including right/left hand/feet that might cause amplitude suppression (*event-related desynchronization* — ERD), amplitude enhancement (*event-related synchronization* — ERS) of (Rolandic)  $\alpha$  rhythm (7-13 Hz) or central  $\beta$  rhythm (13-30 Hz) EEG signals recorded over subject's sensorimotor cortex on the occipital lobes [57]. The subject is trained to control a parachuting game in which his right/left hand MIs correspond to landing the parachutist on right/left landmarks. Without human control, the parachutist lands in 4 seconds. Normally, it takes the user 10 seconds to land the parachutist.

In the signal processing procedure, recorded EEG signals at sampling rate of 512 Hz from 16 electrodes placed over sensorimotor cortex are band-pass filtered by Laplacian spatial

filtering. After time to frequency domain conversion over a PSD timing window of 62.5 ms, 23 frequency components in the range of 4-48 Hz are selected. The spectral features are further dimensionally reduced and extracted using canonical variate analysis for canonical discriminant spatial patterns. *Gaussian mixture model* (GMM) is utilized as the classifier that requires training by reducing the mean square error of distribution parameters with a stopping condition set by the user. Less reliable feedback of this BCI is further processed and enhanced by an *assisting evidence accumulation framework* (AEAF) that mimics an online decision making scheme. The AEAF makes two major contributions to the BCI that are subject brain activation optimization and false positive result elimination. Further details of the Motor Imagery-based BCI paradigm are given in [47, Appendix A].

### 3. Proposed method

In the previous sections, BCIs with different sophisticated configurations are developed for the purposes of mouse cursor movement control, cyber-games play and other control problems. Most BCIs in the literature share a common characteristic to require the EEG signals to be converted into user's intents spontaneously [35, 41]. The previously illustrated BCIs also need extra assistant devices, such as a computer screen or 3D checkerboard graphics, for EEG signature (i.g. P300, SSVEP, etc.) elicitation. Differently, our BCI (see Figure 3) aims at assisting patients to control electronic devices so one expected time epoch to trigger a specific control command is 1~3 minutes since the moment user starts expressing his intent. On one hand, this loose time requirement doesn't affect the user's comfortability by keeping them to be awaited for their intents to be executed. On the other hand, the system has a sufficient time duration to process and give accurate control commands. Non-reliance on external trigger devices for EEG signature capturing reduces the complexity and hence it makes our proposed BCI more feasible for practical implementation.

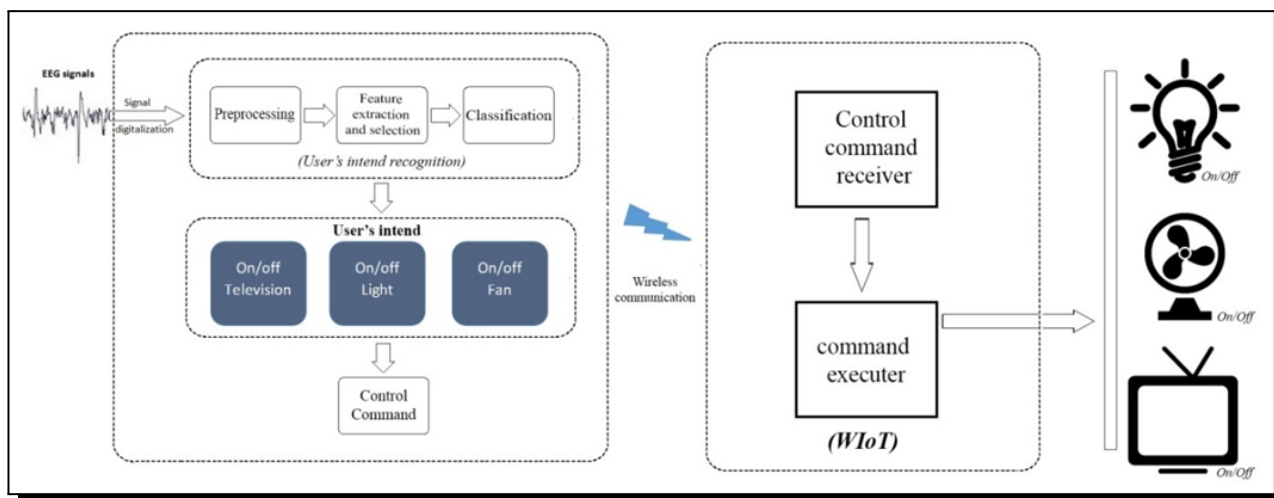


**Figure 3.** A BCI to control electronic devices

The proposed BCI system also consists of a wireless communication block in which a *wireless internet of things* (WIoT) component is integrated into the electronic device and directly operates the device once the command is received. The most important part of our BCI WIoT is a *system on chip* (SoC) ESP 8266 with TCP/IP protocol that allows wireless communication between the Wi-Fi network and WIoT. Once WIoT receives the command, it performs turning on/off operations of the electronic devices with a negligible time delay.

Last but not least, a scheme is proposed based on DNN integrated into our BCI system, capable of processing EEG data and translating user's thoughts into accurate controlling commands. This DNN scheme that ensures reliability, robustness and efficiency for the purpose of our BCI consists of eight stages that are raw signal acquisition, spectral filtering, artifact removal, spectral feature extraction, normalization, dimensionality reduction, principal component selection and classification. Vital stages of the proposed method are described as follows:

### 3.1 Artifact removal

EEG artifacts, mostly caused by eye blinks and movements, muscle movements, chewing and the like, are undesired interferences that cause changes in the signal measurements and affect the signal of interest [54]. Artifact falsifies interpretation of EEG signals' true meaning and degrades the quality of the BCI system. Thus, artifact removal/decontamination is necessary for BCI performance improvement.

ICA/Infomax has remained a benchmark method to remove EEG artifacts [21]. In ICA implementation procedure, a large amount of data and visual inspection to eliminate noisy independent components are required. Wavelet thresholding is also rendered for the same task but it is sensitive to basis wavelet and thresholding function selection that causes its results to be inconsistent [25]. Among methods proposed in the literature for EEG artifact removal [54], *wavelet neural network* (WNN) has proven to be an efficient and stable method to remove EEG artifacts, particularly applicable for online BCIs [38, 40], leading to its selection as an integral part of our proposed approach.

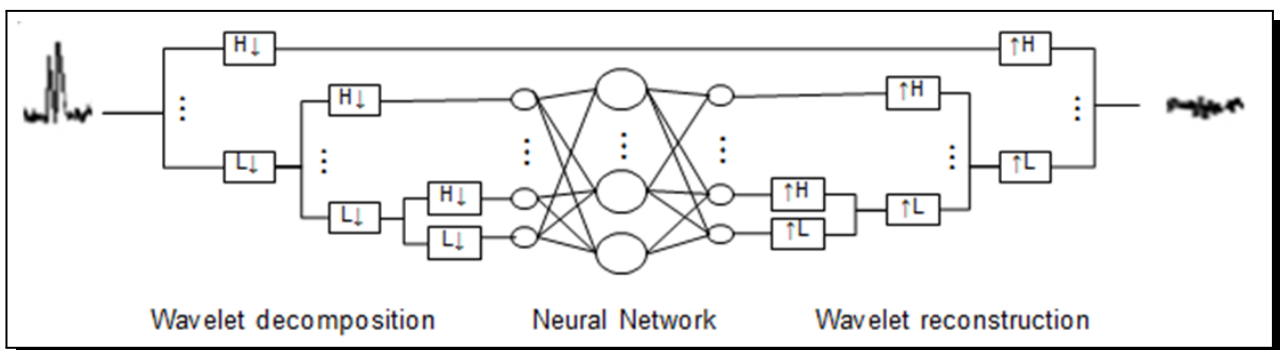


**Figure 4.** Wavelet neural network structure

A WNN comprises of three components, namely wavelet decomposition, an *artificial neural network* (ANN), and wavelet reconstruction (see Figure 4). There are two stages, i.e., training and testing, to implement WNN for artifact removal. In the training stage, simulated EEG signals are generated, real transients/artifacts are added and decomposed with a wavelet transform. A feedforward, fully-connected ANN is trained with low frequency sub-band coefficients. In the testing stage, contaminated EEG signals are wavelet-transformed. A set of low frequency sub-band coefficients are passed through the trained WNN to produce “corrected” corresponding coefficients required for wavelet reconstruction. WNN implemented in this way makes it possible to suppress EEG artifacts, particularly EOG artifacts that are unavoidable due to experimental protocol of the BCI under discussion [40].

### 3.2 Data Dimensionality Reduction

The entire EEG spectrum is not necessary for a good classification result. Spectral features at delta, theta, and some high frequencies in the gamma range are dropped out. The number of remaining features are further reduced by PCA that is implemented with *single value decomposition* (SVD).

PCA is a multivariate statistical technique that is widely applied in various works [1, 24, 45]. By maximizing the scatter of all the projected samples and generating an orthonormal basis vector, PCA transfers the data onto a new coordinate system [24]. This functionality makes it possible to apply PCA to reduce dimensionality of a complex dataset and produce a new dataset of most significant features with simplified structure [20]. Those features are called *principal components* (PCs) that are ranked according to the significance level/data variability denoted by their eigenvalues [2]. In this paper, the number of PCs that needs to be retained for the best performance of the DNN is determined by applying SURE thresholding [60].

The mathematical definition of PCA is given in the following:

Given a sample of  $n$  observations on a vector of  $m$  variables  $\{x_1, x_2, \dots, x_n\} \in \mathcal{R}^m$ , the first principal component of the sample is defined by the linear transformation

$$p_1 = \alpha_1^T x_j = \sum_{i=1}^m \alpha_{i1} x_{ij}, \quad (3.1)$$

where  $j = 1, 2, \dots, n$ , the vectors  $\alpha_i = (\alpha_{i1}, \alpha_{i2}, \dots, \alpha_{im})$  and  $x_j = (\alpha_{1j}, \alpha_{2j}, \dots, \alpha_{mj})$  are selected by maximizing  $p_1$ 's variance. PCA is implemented by different methods including singular value decomposition.

### 3.3 Principal Component Selection

We implement the SURE thresholding method on each subject's data and then select only the PCs whose variances are less than the outcome threshold returned by the method. The final number of PCs to be retained for our BCI is then determined by averaging the number of retained PCs on each subject.

To remove EEG spectral features that are not essential to the DNN classifier, PCA could be applied to lower their dimensionality [50, 51]. Regarding this application, we save computational power and improve performance of the BCI system at the same time. The number of retained PCs could be selected initially with a “hard” value [8, 50, 51]. Our goal is to build a BCI that enables patients with any type of characteristics to communicate efficiently with the surrounding electronic devices, so mostly, the BCI is used by subjects with different characteristics. Therefore, an appropriate number of essential PCs for feature selection needs to be determined adaptively and data-orientedly. In our work, a PC is not removed if its corresponding variance is less than a certain threshold. Among schema for thresholding calculation [9, 11], an adaptive algorithm based on the SURE [12, 52] along with a soft-like thresholding function [60] is selected.

Applying to the selection of PCs, the optimal value of  $t$  can be determined adaptively based on the SURE method as followed

$$t_{i+1} = t_i - \nabla t_i, \quad (3.2)$$

in which the threshold at step  $i$  is calculated as

$$\nabla t_i = \alpha \cdot \frac{\partial R_s(t)}{\partial t}, \quad (3.3)$$

where

$$\frac{\partial R_s(t)}{\partial t} = 2 \sum_{i=0}^{N-1} g_i \cdot \frac{\partial g_i}{\partial t} + 2 \sum_{i=0}^{N-1} \frac{\partial^2 g_i}{\partial p_i \partial t}, \quad (3.4)$$

and

$$g_i = Q(p_i, t) - p_i \quad (3.5)$$

and

$$Q(p, t) = \begin{cases} p + t - \frac{t}{2^{k+1}}, & p < -t \\ \frac{1}{(2^{k+1})t^{2k}} p^{2k+1}, & |p| \leq t \\ p - t + \frac{t}{2^{k+1}}, & p > t \end{cases} \quad (3.6)$$

here,  $k$  is a positive number and  $p$  represents values of PC variances. For a set of  $n$  PCs, the threshold is initialized with Donoho threshold [11] as follows:

$$t_0 = \frac{\text{median}(|p|)}{0.6745} \sqrt{\frac{2 \log(n)}{n}}. \quad (3.7)$$

This process is repeated until  $\nabla t_i / t_{i+1} > \varepsilon$ .

### 3.4 Deep Neural Network Classification

DNN is a deep, multi-layered machine learning model that is capable of performing either classification or regression tasks. Deep learning [17] is a semi-supervised learning scheme which aims at training DNN efficiently and avoiding the over-fitting problem. Deep learning includes two phases: pre-training and fine-tuning. In the first pre-training phase, the *restricted Boltzman machine* (RBM) is utilized in order to initialize the best weight with unlabeled data. In the second fine-tuning phase, the DNN with weight initialized in with pre-training

is trained by the classical back-propagation method with labeled data. Compared to classic learning algorithms, deep learning possesses two major advantages, i.e., generalizing better post-training combination of learned features and composing multiple levels of abstractions with a deep structure that enables a deep net to analyze the features layer by layer with high efficiency [28].

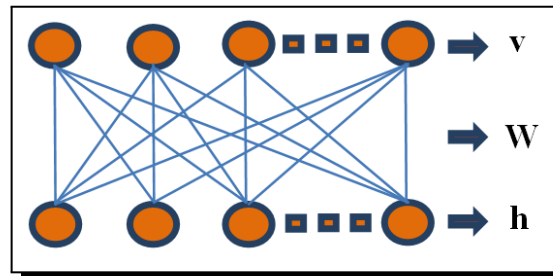


Figure 5. Restricted Boltzman machine

A RBM [48] consists of only two input/visible and output/hidden layers. Units in either visible or hidden layer are not connected layered-internally and they have undirected, symmetrical and full connections from visible to hidden units by a set of weights  $W$ . Both hidden and visible units, defined as  $v \in \{0, 1\}^M$  and  $h \in \{0, 1\}^N$ , respectively, are binary stochastic. Accordingly, the number of elements in  $W$  is  $M \times N$ . The ultimate goal of any unsupervised learning algorithm for RBM is to maximize the probability  $p(v; W)$  which assigns the best-suited set of weights  $W$  to a visible vector  $v$ :

$$p(v; W) = 1/\delta(W) \sum_h \exp(-E(v, h; W)), \tag{3.8}$$

in which  $\delta(W)$  is partition function or normalizing constant, it is defined as

$$\delta(W) = \sum_v \sum_h \exp(-E(v, h; W)), \tag{3.9}$$

where  $E(v, h; W) = -\frac{1}{2}\{v^T W h + \alpha^T v + \beta^T h\}$  with  $\alpha$  and  $\beta$  are bias terms.

Maximizing  $p(v; W)$  equivalent to approaching a suited model is tough. However, there exists an alternative way to do that by taking the following inequality into consideration:

$$\log p(v; W) \geq \sum_h q(h|v) \{\log p(v, h; W)\} + \mathcal{H}(q(h|v)), \tag{3.10}$$

in which  $\mathcal{H}(q(h|v))$  is the entropy functional of the approximating distribution  $q(h|v)$ . Our purpose of finding the best weight to connect visible to hidden units,  $W$  becomes maximizing the lower bound of equation (3.10) by using contrastive divergence learning [18]. This approach is called variational learning which has proven as an efficient solution to pre-training a *DNN/deep belief net* (DBN) (see Figure 6) comprising of various RBMs. The output/hidden units of a single RBM in the previous layer are input/visible units of the RBM in the next layer, respectively. We repeat variational learning  $n$  times for  $n$  hidden layer DBN and while performing variational learning for the  $i^{th}$  RBM out of  $n$ , all the previous RBMs need to be frozen.

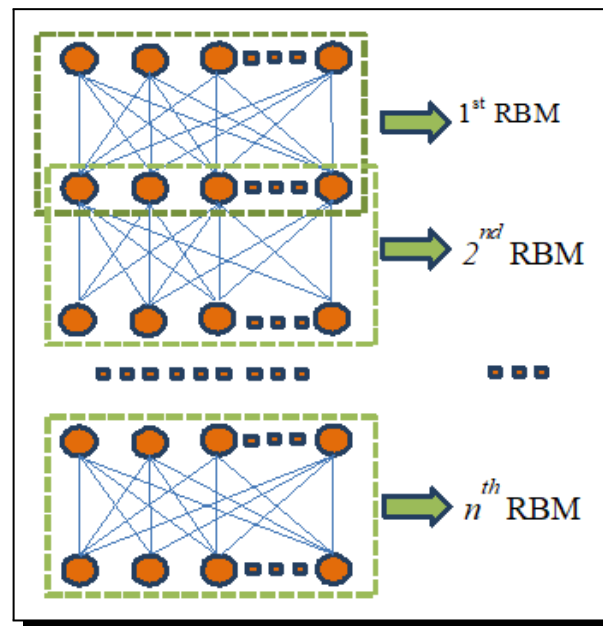


**Figure 6.** Deep neural network with RBMs

In our work, DNNs prove to be an appropriate machine learning model to spectral features selected by PCA and it is capable of classifying non-stationary EEG signals into mental states efficiently.

## 4. Results

In this Section we describe experimental protocol and report experimental results collected during the course of this work implementation.

### 4.1 Experimental Protocol

The proposed method is validated on an EEG dataset [5] recorded from four healthy subjects (age of from 20 to 30) while subjects are asked to turn their minds into Zen condition (almost completely empty – thinking), imagine turning a light on and memorize a sentence extracted from a complicated scientific paper (around ten words each sentence) that are equivalent to three mental tasks Neutral, Light, and Paper, respectively. The subjects remain eye-closed in the Neutral task and eye-opened in the rest tasks. They neither have recent caffeine, food or beverage, nor take any medication at least 24 hours before the recording. Each subject has 2 hours to get familiar with the recording conditions, equipment and task requirements. We record 10 sessions for each subject's mental task and each session lasts 90 seconds. Between two sessions, the subjects are asked to relax for 2 minutes. In total there are 30 EEG data segments (14 (number of channels)  $\times$  90 (duration of one epoch)  $\times$  128 (sampling rate) = 161,280 data samples/one segment) for each subject.

Recording is carried out in an acoustic laboratory room that is well insulated so as to prevent the sounds and lights from the surroundings from distracting the subjects. The subjects remain

silent and are requested to avoid any movements as much as possible during the recording. An Emotiv EPOC+ headset of 14 EEG channels, 2 references and sampling rate at 128 Hz is utilized for signal measurement. The electrodes are placed on the scalp at locations AF3, F7, F3, FC5, T7, P7, O1, O2, P8, T8, FC6, F4, F8, and AF4 as depicted in Figure 7.

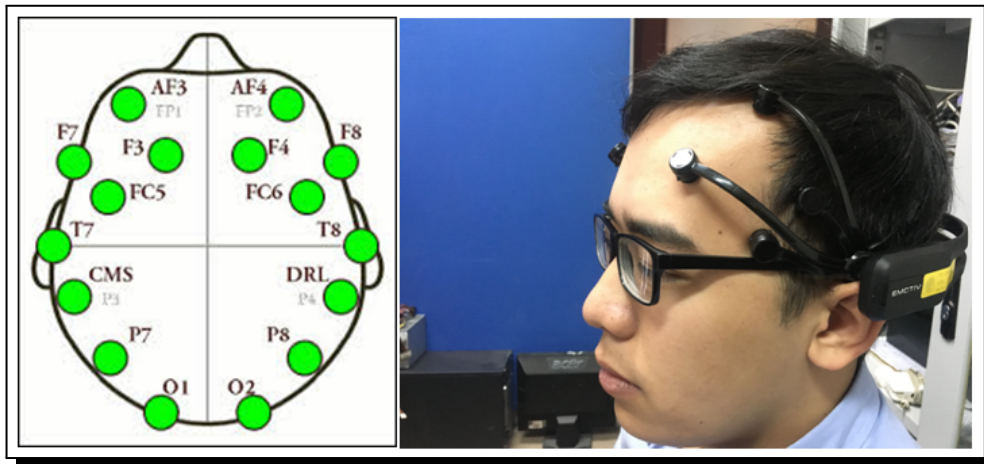


**Figure 7.** Electrode topography and an Emotiv EPOC+ headset

The proposed method is implemented in a computer equipped with regular components (Intel Core i7 8 CPUs (2.6 GHz/CPU) and 16 GB RAM). The EEG signals recorded with the EPOC+ headset are transmitted to the computer via Wi-Fi communication.

## 4.2 Results

In this sub-section, the experimental results regarding EEG artifact-suppression, topographical visualization of neural activation and system performance are reported.

### i. Artifact suppression

Due to the topography of the Emotiv EPOC+ recording session, channels (AF3, AF4, F3, F4, FC5 and FC6) in the frontal region of the scalp are affected most severely by the EEG artifacts. Hence, WNN is implemented mainly on EEG data at these channels to reduce falsification of data interpretation. Wavelet decomposition and wavelet basis function are selected at 6 levels and Coif3, respectively. The ANN consisting of 4 input units, 6 hidden units and 4 output units is trained by output weight *optimization – backpropagation* (OWO - BP). This selection is effective in our experiment as it has been shown in [31].

As illustrated in Figure 8 the correction results of an EEG data segment, the EOG artifacts which resemble the shapes of spikes, that occur randomly, are removed completely while the cerebral information in the background and also at the location that EOG artifacts appear is well-preserved. In the time domain, the amplitude of the EEG samples remain identical before and after the correction which mean that WNN correction doesn't affect the nature of cerebral information that EEG signals carry. WNN is still effective in the case that multiple artifacts appear as shown in Figure 8.

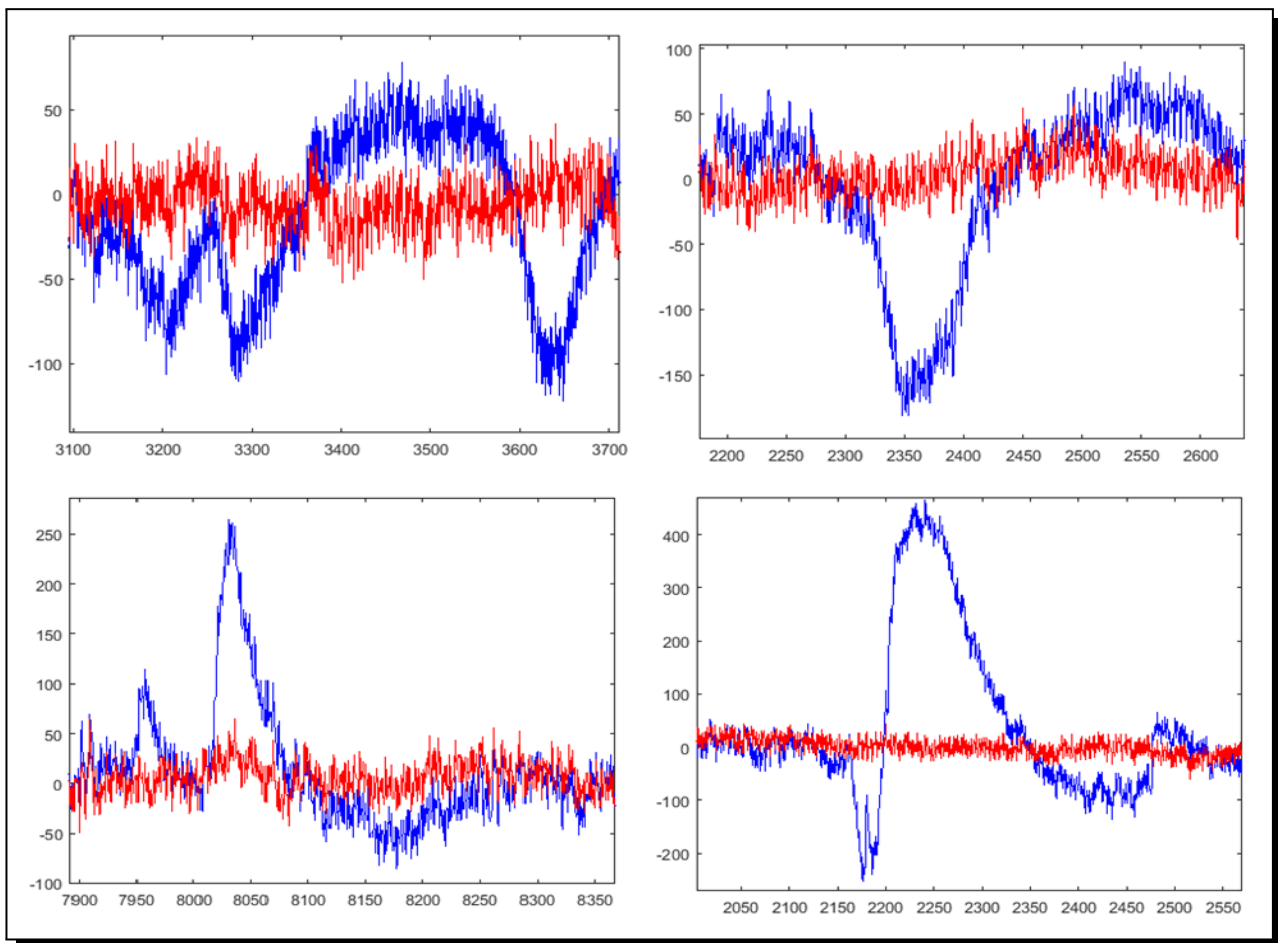


**Figure 8.** Artifact-free EEG data segments (Blue and Red lines correspond to EEG Signals before and after artifact removal)

## ii. Topographical visualization of neural activation

*Low resolution brain electromagnetic tomography* (LORETA) [43,44] is implemented to visualize neural activations over the course of the recording. LORETA utilizes the topography information and raw EEG recordings and calculates current density throughout the human brain. Each specific brain voxel is mapped to a corresponding index of current density. Accordingly, each voxel is then color-coded onto a color encoding bar from white to red that is equivalent to increasing the index from low to high. In Figure 9, we show LORETA images of subject #4 while performing each of the three mental tasks.

## iii. Principal Component Selection

Aimed at obtaining a SURE thresholding that enables to return the corresponding number of PCs to be retained, parts of the proposed method that are stages from 1 to 6 are implemented on EEG data of each subject. After this step, numbers of retained PCs over EEG training data of the four subjects are averaged and it is possible to get the optimal number of PCs applicable to the entire dataset.

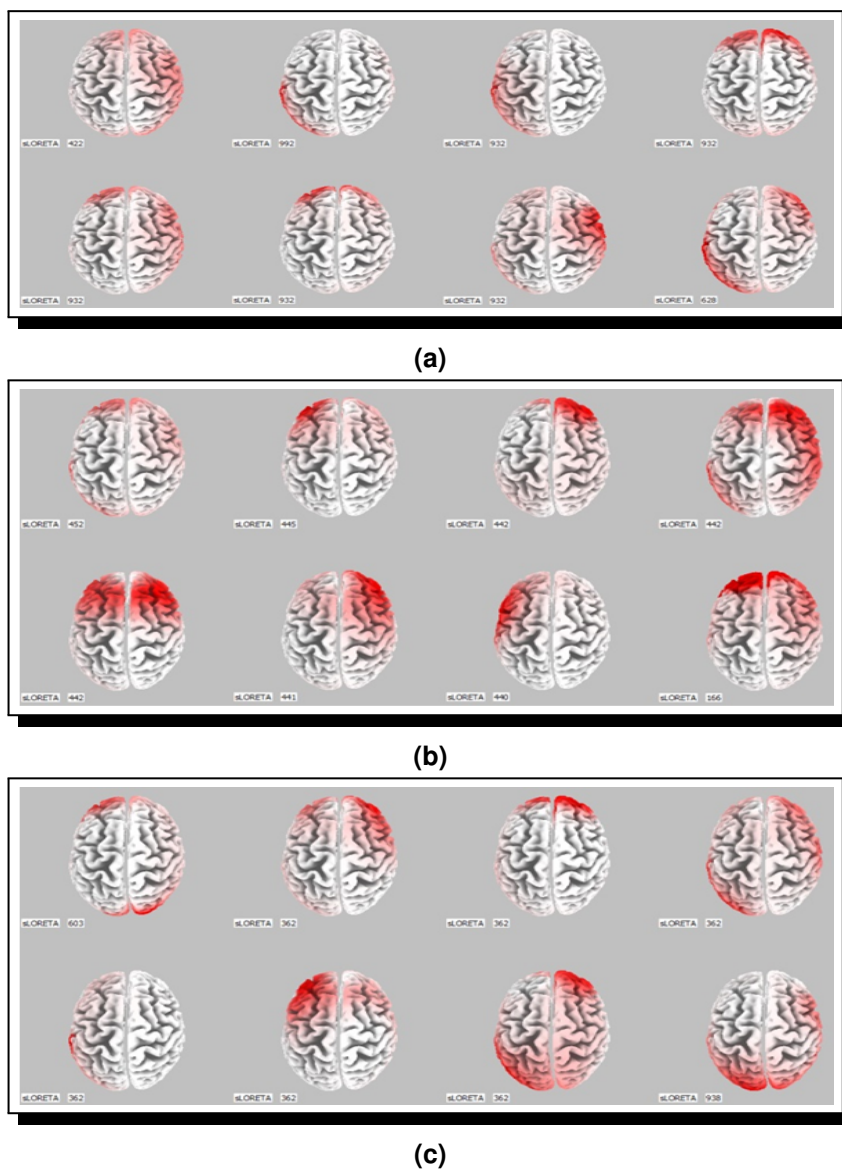


**Figure 9.** Activated regions while a subject is performing three mental tasks (a) Neutral, (b) Paper and (c) Light

For the best performance of SURE thresholding, we set  $\epsilon = 0.0001$ ,  $\alpha = 0.005$  and  $k = 3$ . The optimal number for PCs to be retained in this setting is 13 (see Table 1).

**Table 1.** Sure thresholding for the optimal number of pc

Subject	Threshold value	Number of PCs	The optimal number of retained PCs
#1	1.3797	11	13
#2	0.7750	14	
#3	1.1700	12	
#4	0.2059	15	

iv. System performance

Experimental results regarding system performance are reported. In the dual mental task experiment, we group Light and Paper mental tasks into the same group of non-neutral and Neutral mental task into another. Meanwhile in the triple mental task experiment, EEG signals are categorized into three groups of Neutral, Light and Paper.

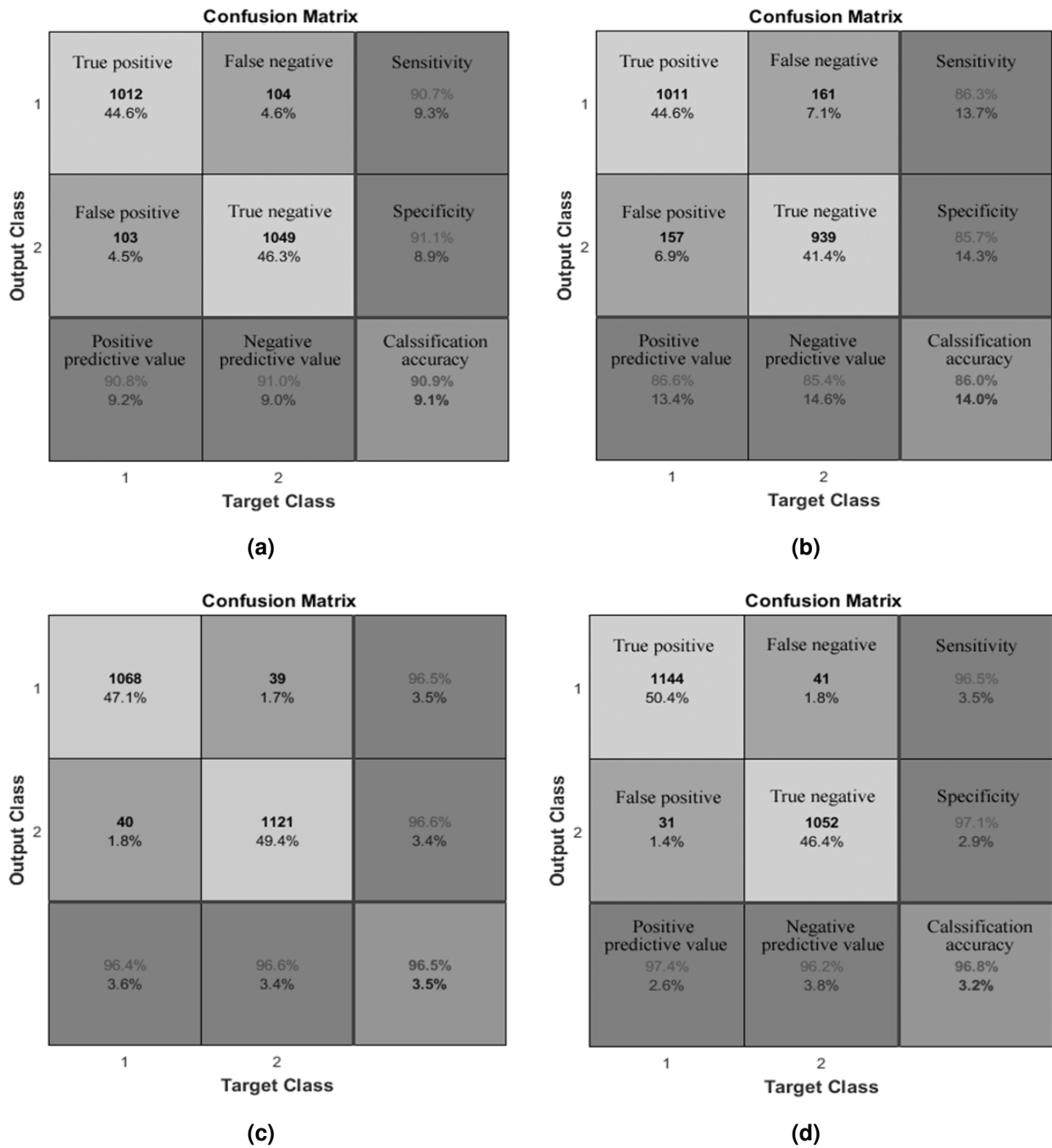


Figure 10. Confusion matrixes of system performance on dual mental task EEG data of subjects #1(a), #2(b), #3(c) and #4(d)

We implement our proposed method along with other methods (NB, LDA, KNN, SVM and ANN) on two types of experiments with dual and triple mental tasks are reported in Table II and III, respectively. For the first four method (NB, LDA, KNN and SVM) implementations, we use entire spectral range of PSD features without artifact removal and dimensionality reduction as input of the classifiers. The setting for ANN method is quite similar to the proposed deep neural network based method in which spectral features in frequency ranges of 0-8 Hz and 50-64 Hz are dropped-out and then dimensionality-reduced from 42 to 10.

**Table 2.** Dual Mental Task Classification Results

Method	Accuracy (%)				
	Subject #1	Subject #2	Subject #3	Subject #4	Average
NB	52.28	40.96	71.19	73.30	59.43
LDA	69.09	65.96	67.80	66.52	67.34
KNN	79.54	62.23	92.80	90.25	81.20
SVM	85.95	80.16	90.28	90.78	86.79
ANN	87.29	82.13	93.95	95.23	89.65
DNN	90.87	<b>85.98</b>	96.52	<b>96.83</b>	<b>92.55</b>

Baseline deep neural network system includes all steps except for WNN and PCA-SURE. It also utilizes spectral features with dimensionality reduced by PCA with a fixed number of PCs to be retained of 10. Then we implement the method by adding WNN and then PCA-SURE to see how they contribute to the overall performance of the proposed system.

**Table 3.** Triple Mental Task Classification Results

Method	Accuracy (%)				
	Subject #1	Subject #2	Subject #3	Subject #4	Average
NB	52.32	55.56	58.68	54.90	55.36
LDA	62.60	61.34	64.89	59.78	62.15
KNN	67.16	63.12	66.25	68.15	66.17
SVM	67.25	71.18	67.27	72.89	69.64
ANN	<b>70.25</b>	73.62	69.94	75.45	72.31
DNN	<b>71.08</b>	75.71	73.19	<b>76.90</b>	<b>74.22</b>

For the proposed method, we use a DNN of structure 15-200-100-20-2/3 (15 input units, three hidden layers of 200, 200 and 200 hidden units and 2/3 output units). Numbers of iterations for pre-training and fine-tuning are set at 200 and 100, respectively. We use 70% and 30% of the entire EEG dataset for training and testing. Within the training set, 30% of the data is used for pre-training and the rest for fine-tuning the Deep Net.

Confusion matrices with evaluation metrics True positive, False negative, False positive, True negative, Sensitivity, Specificity, Positive predictive value, Negative predictive value and Classification Accuracy (the main evaluation metric on system performance for most of our work) are also reported at Fig. 10, where subjects performing dual mental task experiment are analyzed to provide more statistical details.

## 5. Discussion

In this study, our aim is to build a BCI that is capable of executing users' intents to control electronic devices effectively purely with mind power. Such a BCI system is realized by integrating multiple neural engineering techniques in a proper manner. The differences in nature and usage of each technique make such integration not a trivial task. We could see that without a good preprocessing stage, the average classification result is reduced by around 1%. WNN is utilized to remove EOG artifacts in this work but it could be replaced or combined with other techniques for better effect. Furthermore, other types of *artifacts like electromyography (EMG) and electrocardiography (EKG)* are evident in our dataset and if they could be removed, we believe the classification results would be improved significantly. It is also observed that classification results with artifact-free signals are not often higher than the ones with contaminated signals. For example, that happens to the cases of subject #4 and subject #2 for dual and triple mental task experiments, respectively (Table 4 and 5).

**Table 4.** Dual mental state system performance over stages

Method	Accuracy (%)				
	Subject #1	Subject #2	Subject #3	Subject #4	Average
Baseline DNN system	87.89	84.13	94.80	96.35	90.79
+WNN	88.59	85.94	95.45	96.17	91.53
+PCA-SURE	90.87	<b>85.98</b>	96.52	<b>96.83</b>	92.55

The results returned by our proposed method shown at Table 1 and 2 are remarkably better than by other methods. For the proposed method implementation, the highest classification accuracies with dual and triple mental state tasks are achieved for subjects 3 and 4, respectively. These results indicate EEG signals are analyzed differently by the proposed method when the classes are increased. This scenario is equivalent to higher complexity of the mental tasks the subjects need to perform. For both types of experiment, the proposed method performs best with the highest classification accuracies reported on EEG data of subject 4. Meanwhile, the ranking of classification accuracies from low to high of type I and II experiments are not identical. Furthermore, the differences (around 5-6%) between the worst and best classification results with the proposed method among four subjects reveal that the classification results are data-oriented and there exists just a universal model/solution to BCI implementation. This observation could be explained based on the fact that even this experimental protocol makes it

quite convenient for the subjects to follow and run the BCI it is hard for them to produce signals at the identical quality that is well-distinguished to the classifiers.

It could be seen that the classification accuracy for dual mental states is much higher compared to the classification accuracy for triple mental states. The reason might lie in higher complexity of EEG signals in the triple mental state tasks. Besides, there might not be clearly distinguished characteristics of the EEG signals between those mental tasks, i.e., Light and Paper which hinder even the best classifiers to do well. Thus, it is not trivial to come up with an appropriate experimental design in which mental states are well-distinguished.

**Table 5.** Triple mental state system performance over stages

Method	Accuracy (%)				
	Subject #1	Subject #2	Subject #3	Subject #4	Average
Baseline DNN system	69.15	74.92	70.25	74.85	72.29
+WNN	70.68	74.79	72.14	76.24	73.46
+PCA-SURE	<b>71.08</b>	75.71	73.19	<b>76.90</b>	74.22

The confusion matrices show us the data are not unbalanced and the system doesn't produce a high rate of misclassification. There are two points to be noted. First, Type I & II errors, that occur when the classes are assigned inaccurately, are minimal for the case that the system performs on subject #4. Second, Sensitivities and Specificities are inversely proportional (Subjects #1: 90.7% and 8.9%, #2: 86.3% and 14.3%, #3: 96.5% and 3.4%, #4: 96.5% and 2.9%) in the same order as the classification accuracies. These experimental evaluation metrics indicate that the proposed system is reliable and performs best and worst on subjects #4 and #2, respectively. Thus, with this experimental protocol, the system would perform well with subjects who followed the way that subject #4 performed his mental task and should avoid the way that subject #2 performed them.

The proposed approach consists of 8 stages and Table 4 and 5 shows that the two stages with PCA – SURE Thresholding and Deep neural network make significant contributions to improving the performance of the entire system. Compared to the baseline Deep neural network system, additional WNN and PCA-SURE Thresholding stages contribute up to 2% of classification accuracy improvement. On the one hand, PCA – SURE Thresholding provides us a data-oriented and adaptive solution to seeking a suitable number of retained PCs that enables the system to save both computational power and improve its overall performance. Considering Deep neural network is a fairly complicated machine learning model with high computational complexity, this contribution is significant. On the other hand, it has been mentioned that EEG spectral data have non-linear and non-stationary characteristics that make classification difficult for conventional linear and statistical models. Deep neural network with multi-layered structure is applied successfully in this work and it is proved to be a suitable classifier for analyzing EEG data into multiple abstract level and produce remarkably excellent accuracy.

The LORETA images of topographical neural activation show that neural activities take place across all electrode locations of the Emotiv EPOC+ during the course of EEG recording while subjects perform each mental state task (Figure 9). Specifically, at a particular time epoch, only a few regions of the scalp are red which means they are activated and then disappear shortly after that. The activation changes to other regions immediately and the following activated regions are unpredictable. It means that many cerebral activities under the scalp occur over time. Importantly, this observation supports our assumption that EEG signals from all EEG electrodes are informative and necessary to our BCI rather than from a group of electrodes.

## 6. Conclusion

To conclude, we present a novel, robust approach based on deep neural network that is capable of classifying and then translating mental states into control commands effectively. It is possible to realize a BCI to control electronic devices by attacking the problem in this direction. The experimental results show that our proposed approach outperforms other methods. The system performance could be improved by introducing other state-of-the-art feature extraction/selection techniques along with powerful machine learning models to the existing system. Finally, the presented BCI is about to be implemented in a large EEG dataset of diversified subjects for the best system configuration in a near future.

## Acknowledgement

This work was supported by Vietnam Academy of Science and Technology, Vietnam (Grant no. VAST01.03/16-17) and partially supported by project named “Multimedia application tools for intangible cultural heritage conservation and promotion”, project number ĐTDL.CN-34/16 and by FIRST Central Project Management Unit, Ministry of Science and Technology, Vietnam under Grant Agreement number 12/FIRST/2a/IoIT. We thank Emotiv. Inc for providing Emotiv EPOC+ headsets for experimentation.

## Competing Interests

The authors declare that they have no competing interests.

## Authors' Contributions

All the authors contributed significantly in writing this article. The authors read and approved the final manuscript.

## References

- [1] H. Abdi and L.J. Williams, Principal component analysis, *Wiley Interdisciplinary Reviews: Computational Statistics* **2**(4) (2010), 433 – 459, DOI: 10.1002/wics.101.

- [2] D.J. Abson, A.J. Dougill and L.C. Stringer, Using principal component analysis for information-rich socio-ecological vulnerability mapping in Southern Africa, *Applied Geography* **35**(1) (2012), 515 – 524, DOI: 10.1016/j.apgeog.2012.08.004.
- [3] S. Amiri, R. Fazel-Rezai and V. Asadpour, A review of hybrid brain-computer interface systems, *Advances in Human-Computer Interaction* **2013** (2013), 1, DOI: 10.1155/2013/187024.
- [4] C.W. Anderson, E.A. Stolz and S. Shamsunder, Multivariate autoregressive models for classification of spontaneous electroencephalographic signals during mental tasks, *IEEE Transactions on Biomedical Engineering* **45**(3) (1998), 277 – 286, DOI: 10.1109/10.661153.
- [5] N.T. Anh, T.H. Hoang, V.T. Thang and T.Q. Bui, An Artificial Neural Network approach for electroencephalographic signal classification towards brain-computer interface implementation, in *Computing & Communication Technologies, Research, Innovation, and Vision for the Future* (RIVF), 2016 IEEE RIVF International Conference, November 7, 2016, pp. 205 – 210, DOI: 10.1109/RIVF.2016.7800295.
- [6] F. Beverina, G. Palmas, S. Silvoni, F. Piccione and S. Giove, User adaptive BCIs: SSVEP and P300 based interfaces, *PsychNology Journal* **1**(4) (2003), 331 – 354, <http://citeseerx.ist.psu.edu/viewdoc/download?doi=10.1.1.161.3731&rep=rep1&type=pdf>.
- [7] B. Blankertz, K.R. Muller, D.J. Krusienski, G. Schalk, J.R. Wolpaw, A. Schlogl, G. Pfurtscheller, J.R. Millan, M. Schroder and N. Birbaumer, The BCI competition III: Validating alternative approaches to actual BCI problems, *IEEE Transactions on Neural Systems and Rehabilitation Engineering* **14**(2) (2006), 153 – 159, DOI: 10.1109/TNSRE.2006.875642.
- [8] E.M. Braack, B. de Jonge, M.J. van Putten, Reduction of TMS induced artifacts in EEG using principal component analysis, *IEEE Transactions on Neural Systems and Rehabilitation Engineering* **21**(3) (2013), 376 – 382, DOI: 10.1109/TNSRE.2012.2228674.
- [9] S.G. Chang, B. Yu and M. Vetterli, Adaptive wavelet thresholding for image denoising and compression, *IEEE Transactions on Image Processing* **9**(9) (2000), 1532 – 1546, DOI: 10.1109/83.862633.
- [10] S. Chiappa and D. Barber, EEG classification using generative independent component analysis, *Neurocomputing* **69**(7) (2006), 769 – 777, DOI: 10.1016/j.neucom.2005.12.028.
- [11] D.L. Donoho, De-noising by soft-thresholding, *IEEE Transactions on Information Theory* **41**(3) (1995), 613 – 627, DOI: 10.1109/18.382009.
- [12] D.L. Donoho and I.M. Johnstone, Adapting to unknown smoothness via wavelet shrinkage, *Journal of the American Statistical Association* **90**(432) (1995), 1200 – 1224, URL: <https://www.jstor.org/stable/2291512>.
- [13] R. Fazel-Rezai, B.Z. Allison, C. Guger, E.W. Sellers, S.C. Kleih and A. Kübler, P300 brain computer interface: current challenges and emerging trends, *Frontiers in Neuroengineering* **17**(5) (2012), 14, DOI: 10.3389/fneng.2012.00014.
- [14] C. Guger, S. Daban, E. Sellers, C. Holzner, G. Krausz, R. Carablon, F. Gramatica and G. Edlinger, How many people are able to control a P300-based brain-computer interface (BCI)?, *Neuroscience Letters* **462**(1) (2009), 94 – 98.
- [15] C. Guger, Using a brain/computer interface for smart-home control, *PerAdaMagazine Toward Pervasive Adaptation* (2009 July), DOI: 10.1016/j.neulet.2009.06.045.
- [16] M. Hajinoroozi, Z. Mao, T.P. Jung, C.T. Lin and Y. Huang, EEG-based prediction of driver's cognitive performance by deep convolutional neural network, *Signal Processing: Image Communication* **47** (2016), 549 – 555, DOI: 10.1016/j.image.2016.05.018.

- [17] G.E. Hinton and R.R. Salakhutdinov, Reducing the dimensionality of data with neural networks, *Science* **313**(5786) (2006), 504 – 507, DOI: 10.1126/science.1127647.
- [18] G.E. Hinton, S. Osindero, Y.W. Teh, A fast learning algorithm for deep belief nets, *Neural Computation* **18**(7) (2006), 1527 – 1554, DOI: 10.1162/neco.2006.18.7.1527.
- [19] M.R. Hohmann, T. Fomina, V. Jayaram, N. Widmann, C. Förster, J. Just, M. Synofzik, B. Schölkopf, L. Schöls and M. Grosse-Wentrup, A cognitive brain–computer interface for patients with amyotrophic lateral sclerosis, *Progress in Brain Research* **228** (2016), 221 – 239, DOI: 10.1016/bs.pbr.2016.04.022.
- [20] I.T. Jolliffe and J. Cadima, Principal component analysis: a review and recent developments, *Phil. Trans. R. Soc. A* **374**(2065) (2016), 20150202, DOI: 10.1098/rsta.2015.0202.
- [21] J.P. Jung, S. Makeig, C. Humphries, T.W. Lee, M.J. Mckeown, V. Iragui and T.J. Sejnowski, Removing electroencephalographic artifacts by blind source separation, *Psychophysiology* **37**(2) (2000), 163 – 178, DOI: 10.1111/1469-8986.3720163.
- [22] I. Käthner, A. Kübler and S. Halder, Rapid P300 brain-computer interface communication with a head-mounted display, *Frontiers in Neuroscience* **9** (2015), 207, DOI: 10.3389/fnins.2015.00207.
- [23] S.P. Kelly, E.C. Lalor, R.B. Reilly and J.J. Foxe, Visual spatial attention tracking using high-density SSVEP data for independent brain-computer communication, *IEEE Transactions on Neural Systems and Rehabilitation Engineering* **13**(2) (2005), 172 – 178, DOI: 10.1109/TNSRE.2005.847369.
- [24] L. Khedher, J. Ramírez, J.M. Górriz, A. Brahim and F. Segovia, *Alzheimer’s Disease Neuroimaging Initiative, Early diagnosis of Alzheimer’s disease based on partial least squares, principal component analysis and support vector machine using segmented MRI images*, *Neurocomputing* **151** (2015), 139 – 150, DOI: 10.1007/978-3-319-18914-7\_9.
- [25] V. Krishnaveni, S. Jayaraman, L. Anitha and K. Ramadoss, Removal of ocular artifacts from EEG using adaptive thresholding of wavelet coefficients, *Journal of Neural Engineering* **3**(4) (2006), 338, DOI: 10.1088/1741-2560/3/4/011.
- [26] N.S. Kwak, K.R. Müller and S.W. Lee, A lower limb exoskeleton control system based on steady state visual evoked potentials, *Journal of Neural Engineering* **12**(5) (2015), 056009, DOI: 10.1088/1741-2560/12/5/056009.
- [27] E.C. Lalor, S.P. Kelly, C. Finucane, R. Burke, R. Smith, R.B. Reilly and G. Mcdarby, Steady-state VEP-based brain-computer interface control in an immersive 3D gaming environment, *EURASIP Journal on Applied Signal Processing* **2005** (2005), 3156 – 3164, DOI: 10.1155/ASP.2005.3156.
- [28] Y. LeCun, Y. Bengio and G. Hinton, Deep learning, *Nature* **521**(7553) (2015), 436 – 444, DOI: 10.1038/nature14539.
- [29] R. Leeb, S. Perdakis, L. Tonin, A. Biasiucci, M. Tavella, M. Creatura, A. Molina, A. Al-Khodairy, T. Carlson and J.D. Millán, Transferring brain–computer interfaces beyond the laboratory: successful application control for motor-disabled users, *Artificial Intelligence in Medicine* **31**(59) (2013), 121 – 132, DOI: 10.1016/j.artmed.2013.08.004.
- [30] C.T. Lin, B.S. Lin, F.C. Lin and C.J. Chang, Brain computer interface-based smart living environmental auto-adjustment control system in UPnP home networking, *IEEE Systems Journal* **8**(2) (2014), 363 – 370, DOI: 10.1109/JSYST.2012.2192756.
- [31] Z. Lin, C. Zhang, W. Wu and X. Gao, Frequency recognition based on canonical correlation analysis for SSVEP-based BCIs, *IEEE Transactions on Biomedical Engineering* **54**(6) (2007), 1172 – 1176, DOI: 10.1109/TBME.2006.889197.

- [32] F. Lotte, M. Congedo, A. Lécuyer, F. Lamarche and B. Arnaldi, A review of classification algorithms for EEG-based brain–computer interfaces, *Journal of Neural Engineering* **4**(2) (2007), R1, DOI: 10.1088/1741-2560/4/2/R01.
- [33] N. Lu, T. Li, X. Ren and H. Miao, A deep learning scheme for motor imagery classification based on restricted boltzmann machines, *IEEE Transactions on Neural Systems and Rehabilitation Engineering* August 17, 2016, DOI: 10.1109/TNSRE.2016.2601240.
- [34] G.R. Müller-Putz, R. Scherer, C. Brauneis and G. Pfurtscheller, Steady-state visual evoked potential (SSVEP)-based communication: impact of harmonic frequency components, *Journal of Neural Engineering* **2**(4) (2005), 123, DOI: 10.1088/1741-2560/2/4/008.
- [35] D.J. McFarland, D.J. Krusienski, W.A. Sarnacki and J.R. Wolpaw, Emulation of computer mouse control with a noninvasive brain-computer interface, *Journal of Neural Engineering* **5**(2) (2008), 101, DOI: 10.1088/1741-2560/5/2/001.
- [36] M. Middendorf, G. McMillan, G. Calhoun and K.S. Jones, Brain-computer interfaces based on the steady-state visual-evoked response, *IEEE Transactions on Rehabilitation Engineering* **8**(2) (2000), 211 – 214, URL: <https://www.ncbi.nlm.nih.gov/pubmed/10896190>.
- [37] J.D. Millán, F. Renkens, J. Mouriño and W. Gerstner, Brain-actuated interaction, *Artificial Intelligence* **159**(1-2) (2004), 241 – 259, DOI: 10.1016/j.artint.2004.05.008.
- [38] J. Minguillon, M.A. Lopez-Gordo and F. Pelayo, Trends in EEG-BCI for daily-life: Requirements for artifact removal, *Biomedical Signal Processing and Control* **31** (2017), 407 – 418, DOI: 10.1016/j.bspc.2016.09.005.
- [39] G.R. Muller-Putz and G. Pfurtscheller, Control of an electrical prosthesis with an SSVEP-based BCI, *IEEE Transactions on Biomedical Engineering* **55**(1) (2008), 361 – 364, DOI: 10.1109/TBME.2007.897815.
- [40] H.A. Nguyen, J. Musson, F. Li, W. Wang, G. Zhang, R. Xu, C. Richey, T. Schnell, F.D. McKenzie and J. Li, EOG artifact removal using a wavelet neural network, *Neurocomputing* **97** (2012), 374 – 389, DOI: 10.1016/j.neucom.2012.04.016.
- [41] A. Nijholt, D. Tan, B. Allison, J. del R. Milan and B. Graimann, Brain-computer interfaces for HCI and games, in *CHI'08 Extended Abstracts on Human Factors in Computing Systems*, pp. 3925 – 3928 (2008), DOI: 10.1145/1358628.1358958.
- [42] S.M. Park, T.J. Lee and K.B. Sim, Heuristic feature extraction method for BCI with harmony search and discrete wavelet transform, *International Journal of Control, Automation and Systems* **14**(6) (2016), 1582 – 1587, DOI: 10.1007/s12555-016-0031-9.
- [43] R.D. Pascual-Marqui, Discrete, 3D distributed, linear imaging methods of electric neuronal activity, Part 1: exact, zero error localization, arXiv preprint <https://arxiv.org/abs/0710.3341>, October 17, 2007.
- [44] R.D. Pascual-Marqui, Review of methods for solving the EEG inverse problem, *International Journal of Bioelectromagnetism* **1**(1) (1999), 75 – 86, URL: <http://www.brainmaster.com/software/pubs/brain/loreta/TechnicalDetails.pdf>.
- [45] S. Pyatykh, J. Hesser and L. Zheng, Image noise level estimation by principal component analysis, *IEEE Transactions on Image Processing* **22** (2013), 687 – 699, DOI: 10.1109/TIP.2012.2221728.
- [46] B. Rebsamen, E. Burdet, C. Guan, H. Zhang, C.L. Teo, Q. Zeng, C. Laugier, M.H. Ang Jr. Controlling a wheelchair indoors using thought, *IEEE Intelligent Systems* **22**(2) (2007), DOI: 10.1109/MIS.2007.26.

- [47] S. Saeedi, R. Chavarriaga and J.D. Millán, Long-term stable control of motor-imagery BCI by a locked-in user through adaptive assistance, *IEEE Transactions on Neural Systems and Rehabilitation Engineering* **25**(4) (2017), 380 – 391, DOI: 10.1109/TNSRE.2016.2645681.
- [48] R. Salakhutdinov and G. Hinton, Deep boltzmann machines, in *Artificial Intelligence and Statistics*, 448 – 455 (2009), URL: <http://proceedings.mlr.press/v5/salakhutdinov09a/salakhutdinov09a.pdf>.
- [49] G. Schalk, D.J. McFarland, T. Hinterberger, N. Birbaumer and J.R. Wolpaw, BCI2000: a general-purpose brain-computer interface (BCI) system, *IEEE Transactions on Biomedical Engineering* **51**(6) (2004), 1034 – 1043, DOI: 10.1109/TBME.2004.827072.
- [50] L.C. Shi, R.N. Duan and B.L. Lu, A robust principal component analysis algorithm for EEG-based vigilance estimation, in *Engineering in Medicine and Biology Society (EMBC)*, 2013 35th Annual International Conference of the IEEE, July 3, 2013, pp. 6623 – 6626, DOI: 10.1109/EMBC.2013.6611074.
- [51] S. Siuly and Y. Li, Designing a robust feature extraction method based on optimum allocation and principal component analysis for epileptic EEG signal classification, *Computer Methods and Programs in Biomedicine* **119**(1) (2015), 29 – 42, DOI: 10.1016/j.cmpb.2015.01.002.
- [52] C.M. Stein, Estimation of the mean of a multivariate normal distribution, *The Annals of Statistics* **1** (1981), 1135 – 1151, URL: <https://projecteuclid.org/euclid.aos/1176345632>.
- [53] Y.R. Tabar and U. Halici, A novel deep learning approach for classification of EEG motor imagery signals, *Journal of Neural Engineering* **14**(1) (2016), 016003, DOI: 10.1088/1741-2560/14/1/016003.
- [54] J.A. Urigüen and B. Garcia-Zapirain, EEG artifact removal—state-of-the-art and guidelines, *Journal of Neural Engineering* **12**(3) (2015), 031001, DOI: 10.1088/1741-2560/12/3/031001.
- [55] A. Vallabhaneni, T. Wang and B. He, Brain-computer interface, in: *Neural Engineering 2005* (pp. 85-121), Springer, US, Optoelectronics & Advanced Materials **8**, 1377 (2006), DOI: 10.1007/0-306-48610-5\_3.
- [56] J.R. Wolpaw, N. Birbaumer, W.J. Heetderks, D.J. McFarland, P.H. Peckham, G. Schalk, E. Donchin, L.A. Quatrano, C.J. Robinson and T.M. Vaughan, Brain-computer interface technology: a review of the first international meeting, *IEEE Transactions on Rehabilitation Engineering* **8**(2) (2000), 164 – 173, <https://www.ncbi.nlm.nih.gov/pubmed/10896178>.
- [57] F.Z. Yetkin, R.A. Papke, L.P. Mark, D.L. Daniels, W.M. Mueller and V.M. Haughton, Location of the sensorimotor cortex: functional and conventional MR compared, *American Journal of Neuroradiology* **16**(10) (1995), 2109 – 2113, DOI: <https://www.ncbi.nlm.nih.gov/pubmed/8585502>.
- [58] M.H. Zarifia, N.K. Ghalehjogh and M. Baradaran-nia, A new evolutionary approach for neural spike detection based on genetic algorithm, *Expert Systems with Applications* **42**(1) (2015), 462 – 467, DOI: 10.1016/j.eswa.2014.07.038.
- [59] T. Zeyl, E. Yin, M. Keightley and T. Chau, Adding real-time Bayesian ranks to error-related potential scores improves error detection and auto-correction in a P300 speller, *IEEE Transactions on Neural Systems and Rehabilitation Engineering* **24**(1) (2016), 46 – 56, DOI: 10.1109/TNSRE.2015.2461495.
- [60] X.P. Zhang and M.D. Desai, Adaptive denoising based on SURE risk, *IEEE Signal Processing Letters* **5**(10) (1998), 265 – 267, DOI: 10.1109/97.720560.